Pollution and Environment (PE)

DOI: http://doi.org/10.7508/pe.01.2024.01.09

ISSN: 2377-5378 (Print)
ISSN: 2377-8148 (Online)
CODEN : PEONAW

ARTICLE

DEVELOPMENT AND IMPLEMENTATION OF SMART CONFIGURATION STRATEGIES FOR DISTRIBUTED ENERGY SYSTEMS THROUGH DUAL-LAYER COOPERATIVE OPTIMIZATION

Jiajin Zhuo

International Energy College, Jinan University, Zhuhai 519070, China
****Corresponding Author E-mails: zjj152181271391@outlook.com***

ARTICLE DETAILS

Article History:

Received 3 January 2024
Accepted 8 March 2024
Available online 13 March 2024

ABSTRACT

With the proposal of "carbon peak, carbon neutral" dual-carbon goals, China's energy supply is facing the problem of cleaner and smarter transformation. To maximize the economic, energy efficiency, and environmental benefits of distributed energy systems to meet the economic, energy-saving, and environmental protection needs of end-users, this research builds a distributed hybrid cogeneration system based on the Proton Exchange Membrane Fuel Cell(PEMFC) as the main body of the study and establishes a multi-objective optimization model through the two-layer collaborative optimization method by combining the NSGA-II algorithm with the genetic algorithm, and the optimal solution set for the economic and environmental objectives is obtained by the NSGA-II algorithm in the upper layer. The NSGA-II algorithm and genetic algorithm are combined, the upper layer of the NSGA-II algorithm derives the optimal solution set for the economic and environmental objectives, the lower layer of the NSGA-II algorithm derives the optimal body for the energy-saving objective by taking the upper solution set as the initial population, and then the loop iteration is realized, and the optimal solution is selected by the TOPSIS method at last, so as to optimally configure the capacity of each component of energy system. This proposes a scientific, efficient and rational design optimization method for the construction and component equipping of distributed energy system. Finally, through the system optimization analysis, it can be seen that the optimally designed energy system is more diversified and superior compared with the traditional scheme. The optimized solution improves the overall performance and stability of the system, and can reduce energy saving and emission reduction expenditures, which brings more economic and environmental benefits to the users.

KEYWORDS

Distributed energy system; two-layer collaborative optimization; NSGA-II; GA; PEMFC

1. INTRODUCTION

As the global population and economy grow, the demand for energy is rapidly increasing, leading to the depletion of traditional energy sources. Additionally, environmental pollution and climate change are becoming increasingly pressing issues. Distributed energy systems are attracting attention because of their flexibility and reliability, but they need to address high costs and energy management challenges. Therefore, rational system optimization schemes need to be designed to enhance their economic, energy efficiency and environmental benefits.

For distributed energy research mainly focuses on system modeling, simulation and analysis, optimization planning, and operation control [1, 2]. Regarding the optimization of distributed energy systems, solution algorithms and optimization objectives have been the focus of research. Kamel et al. came out with a multi-objective optimization model of equipment capacity considering economic, environmental and energy objectives simultaneously, combining genetic algorithm and entropy weight method for solving [3]. Cha et al. introduced MO-MFEA into hybrid power generation system with the optimization objectives of operation economic efficiency, safety and environmental efficiency to discover the implied consistency factors in the optimization problem, so as to improve the optimization effect and efficiency of hybrid power generation system [4]. Yang et al. established an energy system scheduling model based on the Improved Gray Wolf Optimization (IGWO) algorithm for the economic cost problem, and used Tent mapping and nonlinear adjustment strategy optimization algorithm to improve the performance index [5]. Although there has been some progress in multi-objective optimization of distributed energy systems, a single model is mostly used, which is easy to fall into the local optimal solution, especially in the complex multi-objective space, and it is difficult to obtain a better global solution. Therefore, more flexible methods need to be explored to cope with the nonlinear and nonconvex optimization challenges that are difficult to cope with by a single model and to improve the computational efficiency.

Addressing the challenges in optimizing distributed energy systems, two-layer collaborative optimization emerges as a potent strategy, leveraging multiple optimization techniques for effective hierarchical and multi-objective optimization. Recent explorations have introduced innovative methods and algorithms enhancing this domain. For instance, Jiang and colleagues devised a method for Combined Cooling,

Heating and Power (CCHP) systems, employing the NSGA-II algorithm for capacity determination and robust modeling for optimization of operations [6]. Bian's team developed a model prioritizing economy and reliability, with operational reliability quantification at its core [7]. Dong Lei's research proposed a novel approach integrating intelligent switching and dynamic network reconfiguration, utilizing reinforcement learning for complex problem-solving [8].

Despite advancements, existing methods encounter limitations with large-scale and high-dimensional challenges, primarily due to computational demands. Moreover, there's a notable gap in research focusing on the integrated consideration of environmental, economic, and carbon emission objectives in multi-objective, two-layer optimization frameworks.

This study introduces a two-layer collaborative optimization strategy aimed at optimizing capacity allocation within a hydrogen-based hybrid energy system, addressing economic, environmental, and energy efficiency goals. The methodological innovation lies in the synergistic use of the NSGA-II algorithm and genetic algorithms, markedly reducing computational complexity and enhancing adaptability. This approach not only offers a novel path for multi-objective optimization in distributed energy systems but also emphasizes hydrogen as a zero-emission, high-density, and long-term energy storage solution, positioning it at the forefront of sustainable energy storage and distribution strategies.

2. DISTRIBUTED ENERGY SYSTEMS ANALYSIS

2.1 Distributed energy system rchitecture nalysis

The hydrogen-fueled fuel cell industry has emerged as a focal point of development in recent years, with fuel cells offering an efficient way to convert the chemical energy from fuel and oxidizer directly into electrical energy. Unlike traditional energy conversion methods, fuel cells are not constrained by Carnot cycle efficiency limits, boasting high energy conversion efficiency, rapid load response, low emissions, stability, environmental friendliness, low noise, and high reliability. This paper focuses on a distributed energy system centered around the proton exchange membrane fuel cell (PEMFC) as the primary cogeneration power unit. It integrates additional heat and power sources to reliably supply electricity, hot water, and heating to meet residential energy demands.

The system comprises the energy supply, conversion, storage, and demand sides. It integrates solar photovoltaic (PV) panel, wind turbine (WT), electrolysis tank, PEMFC, solar collector (SC), and air source heat pump (ASHP) into a cohesive hybrid cogeneration framework. The energy supply is primarily sourced from wind and solar energy, which, after conversion and storage, is used to fulfill electrical and thermal loads. The operational principle is as follows: excess renewable energy is converted into hydrogen via an electrolysis tank and stored. This hydrogen then powers the PEMFC to generate electricity when needed. Surplus electricity can be sold to the grid, and additional power can be purchased if the demand exceeds the system's capacity. For heating, solar collectors directly warm water in a tank, with the ASHP providing supplemental heat when necessary. This integrated approach ensures a stable, efficient, and environmentally friendly energy supply for residential needs.

2.2 Modeling of distributed energy system

2.2.1 Solar collector

Solar collectors are used to produce heat by absorbing heat during the time period when solar radiation is available. The quantity of heat generated by a solar collector is influenced by solar irradiance and the surrounding temperature. Additionally, the total output power of a solar collector, encompassing any heat losses incurred by the collector, can be mathematically represented by equation (1).

$$Q_{SC} = A_{SC} * (F_R * (\tau\alpha) * G - F_R * U_{sc} * (T_{sc} - T_{en})) \quad (1)$$

2.2.2 Solar photovoltaic cell

Solar photovoltaic cell can convert light resources into electricity output to supply distributed energy systems as renewable energy generators. Solar photovoltaic power generation can be calculated using equations (2-3) in references [9-10].

$$P_{pv} = P_{spv} * \frac{G}{1000} * [1 + \gamma_{pv} * (T_{bat} - 25)] \quad (2)$$

$$T_{bat} = T_{en} + \frac{NOCT - 20}{800} * G \quad (3)$$

2.2.3 Wind turbine

The power output of wind turbine depends on the instantaneous wind speed and can be determined through equations (4-6) [11].

$$\begin{cases} P_{wt} = 0 & v \le V_{ci} \ or \ v \ge V_{co} \\ P_{wt} = \alpha * v^3 - \beta * P_r & V_{ci} < v < V_r \\ P_{wt} = P_r & V_r \le v < V_{co} \end{cases} \quad (4)$$

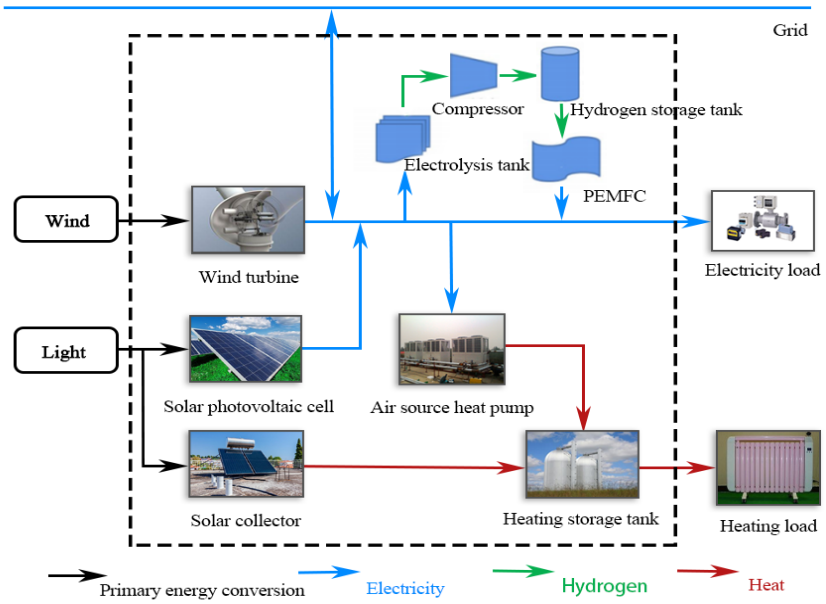

Figure 1. System framework for distributed energy system.

$$\begin{cases} \alpha = P_r / (V_r^3 - V_{ci}^3) \\ \beta = V_{ci}^3 / (V_r^3 - V_{ci}^3) \end{cases} \quad (5)$$

$$P_r = \frac{1}{2} * A_{wt} * C_p * \rho_a * \eta_{wt} * V_r^3 \quad (6)$$

2.2.4 Fuel cell systems (PEMFC)

(1) Electrolysis tank

An electrolysis tank is a device that converts water into hydrogen to be used for energy storage when there is an excess of electricity generated from solar or wind. The chemical reaction in the electrolysis tank is given in equation (7) [12].

$$H_2O + electricity \rightarrow H_2 + \frac{1}{2}O_2 \quad (7)$$

The speed of hydrogen generation in the electrolysis tank can be calculated using equation (8-9) [13].

$$M_{H_2}^{in} = \frac{2P_{elz}}{F * U_{elz}} \quad (8)$$

$$\eta_{elz} = \frac{1.25}{U_{elz}} \quad (9)$$

(2) Compressor

The compressor is used to pressurize the hydrogen produced in the electrolysis tank so that it can be stored in the hydrogen storage tank. The compressor maintains the hydrogen storage tank at the design specified pressure by consuming electrical power. The power consumption of the compressor can be calculated using equation (10).

$$P_c = c_p * \frac{T_c}{\eta_c} * (r_c^{\frac{k-1}{k}} - 1) * M_{H_2}^{in} \quad (10)$$

(3) Hydrogen storage tank

The hydrogen storage tank is used to store hydrogen produced in the electrolysis tank for energy storage. The mass of hydrogen in the hydrogen storage tank can be calculated using equation (11).

$$M_{tank}(t) = M_{tank}(t-1) + M_{H_2}^{in} - M_{H_2}^{out} \quad (11)$$

The volume of hydrogen stored at the design pressure can be calculated using equation (12).

$$V_{H_2} = \frac{M_{tank} * T_{tank} * R}{P_{tank}} \quad (12)$$

(4) Proton exchange membrane fuel cell (PEMFC)

In PEMFC, hydrogen is burned to produce water and electricity. Hydrogen is first decomposed into hydrogen ions at the anode, and then water is synthesized with oxygen at the cathode. The chemical reaction equation is shown in (13-15)[14, 15]

$$H_2 \rightarrow 2H^+ + 2e^- \quad (13)$$

$$2H^+ + 2e^- + \frac{1}{2}O_2 \rightarrow H_2O \quad (14)$$

$$H_2 + \frac{1}{2}O_2 \rightarrow H_2O \quad (15)$$

The output voltage of the PEMFC consists of four components: the nernst voltage (Unernst), the resistive voltage drop caused by the resistor (Uohimic), the activation polarization voltage drop (Uactivition), and the concentration drop (Uconcentration)[16-17], which can be calculated by equation (16), and these four components can be calculated by equations. (17-20), respectively.

$$U_{FC} = U_{nernst} - U_{ohimic} - U_{activition} - U_{concentration} \quad (16)$$

U_{nernst} is calculated as follows[18]:

$$U_{nernst} = 1.229 - 8.5 * 10^{-4} * (T_{FC} - T_{ref}) + 4.3085 * 10^{-5} * T_{FC} * [ln(P_{H_2})] + 0.5 * ln(P_{O_2})] \quad (17)$$

$$P_{H_2} = 0.5 * P_{H_2O} * (\frac{1}{exp(\frac{1.653 * i_{FC}}{T_{FC}^{1.334}}) * x_{H_2O}^{sat}} - 1) \quad (18)$$

$$P_{O_2} = P_{FC} * [1 - x_{H_2O}^{sat} - x_{other\ gases}^{channel} * exp(\frac{0.291 * i_{FC}}{T_{FC}^{0.832}})] \quad (19)$$

$$x_{H_2O}^{sat} = \frac{P_{H_2O}}{P_{FC}} \quad (20)$$

$$log_{10}^{P_{H_2O}} = -2.179 + 0.02253 * (T_{FC} - 273.15) - 9.183 * (10^{-5}) * (T_{FC} - 273.15)^2 + 1.4454 * 10^{-7} * (T_{FC} - 237.15)^3 \quad (21)$$

$$x_{other\ gases}^{channel} = \frac{x_{other\ gases}^{in,ham} - x_{other\ gases}^{out,ham}}{ln(\frac{x_{other\ gases}^{in,ham}}{x_{other\ gases}^{out,ham}})} \quad (22)$$

$$x_{other\ gases}^{in,ham} = 0.79 * (1 - x_{H_2O}^{sat}) \quad (23)$$

$$x_{other\ gases}^{out,ham} = \frac{1 - x_{H_2O}^{sat}}{1 + \frac{\lambda_{air}^{-1}}{\lambda_{air}} * \frac{0.21}{0.79}} \quad (24)$$

U_{ohimic} can be expressed as equation (25) [19]:

$$U_{ohimic} = i_{FC} * R_{internal} \quad (25)$$

Where, $R_{internal}$ is the internal resistance of the PEMFC, which is related to ρ, D, S. ρ is the resistivity of the proton exchange membrane, D is the thickness of the proton exchange membrane and S is the effective working area of the proton exchange membrane. It can be calculated from equation (26-27).

$$R_{internal} = \frac{\rho * D}{S} \quad (26)$$

$$\rho = \frac{181.6 * \left[1 + 0.03 * i_{FC} + 0.062 * i_{FC}^{2.5} * (\frac{T_{FC}}{3.03})^2\right]}{[23 - 0.634 - 3 * i_{FC}] * exp\left(4.18 * (\frac{T_{FC} - 303}{T_{FC}})\right)} \quad (27)$$

$U_{activition}$ can be expressed as:

$$U_{activition} = -\left[\zeta_1 + \zeta_2 * T_{FC} + \zeta_3 * T_{FC} * ln(C_{O_2}) + \zeta_4 * T_{FC} * ln(i_{FC})\right] \quad (28)$$

$$C_{O_2} = \frac{P_{O_2}}{5.08 * 10^6 * exp(-\frac{498}{T_{FC}})} \quad (29)$$

$U_{concentration}$ can be expressed as [20]:

$$U_{concentration} = m * exp(n_{FC} * i_{FC}) \quad (30)$$

$$m = 1.1 * 10^{-4} - 1.2 * 10^{-6} * (T_{FC} - 273.15) \quad (31)$$

The hydrogen consumption rate $M_{H_2}^{out}(g/s)$ during the PEMFC reaction can be calculated by equation (32). Where P_{FC} is the output power of the fuel cell, U_{FC} is the open-circuit voltage, η_{FC} is the fuel cell efficiency and F is the Faraday constant. The output power can be calculated by equation (33).

$$M_{H_2}^{out} = \frac{P_{FC}}{\frac{1}{2} * U_{FC} * \eta_{FC} * F} \quad (32)$$

$$P_{FC} = I_{FC} * U_{FC} * \eta_{FC} \quad (33)$$

$$I_{FC} = i_{FC} * A \quad (34)$$

Where, I_{FC} and n_{FC} are the current during the fuel cell reaction and the

number of fuel cell blocks. A is the area of the fuel cell proton exchange membrane.

2.2.5 Air source heat pump

An air source heat pump (ASHP) is an electrically powered heating unit that absorbs low-temperature heat energy from the air through an evaporator and transfers that energy to a circulating medium. Next, a compressor is used to compress the medium into high-temperature vapors, and the heat from these high-temperature vapors is released into a water tank. In this way, the ASHP continuously extracts heat energy from the air to provide the user with the heat they need. The amount of heat generated by the ASHP can be calculated by equations (35-36).

$$Q_{ASHP} = COP * P_{ASHP} * \varepsilon \tag{35}$$

$$COP = \alpha * T_{en}^2 + \beta * T_{en} + \gamma \tag{36}$$

2.2.6 Heat storage tank

In this study, it is assumed that the temperature in the heat storage tank is homogeneously distributed. Based on the second law of thermodynamics and considering the heat loss of the tank, the model of the tank at time t can be expressed as equation (2-37):

$$T_{tank}(t) - T_{tank}(t-1) = \frac{\Delta t}{c * \rho_w * V_{tank}} * (Q_{ASHP} + Q_{SC} - Q_{loss}) \tag{37}$$

$$Q_{loss} = U_{loss} * A_{tank} * (T_{tank}(t) - T_{en}) \tag{38}$$

$$V_{tank} = A_{tank} * h_{tank} \tag{39}$$

3. DESIGN OPTIMIZATION OF DISTRIBUTED ENERGY SYSTEM

3.1. System operation otrategy

This thesis research focuses on the distributed hybrid cogeneration system, which contains two major systems, power supply and heat supply, and its core objective is to satisfy both power and heat demand and ensure smooth operation of the system.

3.1.1 Heat system operation strategy

In the case of the heat system, the operation strategy is shown in Fig. 2. When the temperature of the heat storage tank exceeds 90°C, it indicates overheating, necessitating the shutdown of the solar collector. Between 60°C and 90°C, the tank operates at a normal temperature, allowing the solar collector to function normally for heat storage. If the tank temperature dips below 60°C, indicating insufficient heat to meet demand, the air source heat pump must be activated to generate heat. It is important to note that the use of an ASHP increases the electrical demand of the system. Therefore, the power consumption of the air source heat pump is included in the operation of the electricity system.

3.1.2. Electricity system operation strategy

The operational strategy for the power supply system is illustrated in

Parameter description

A_{SC} Area covered by solar collectors, m^3

F_R Solar collector heat transfer coefficient, dimensionless

$\tau\alpha$ Effective projected absorptive product of solar collectors, dimensionless

U_{sc} Heat loss coefficient of solar collector, W/(m²·℃)

T_{sc} Surface temperature of solar collector, ℃

T_{en} Ambient temperature, ℃

G Solar radiation, W/m²

γ_{pv} Solar photovoltaic cell power temperature coefficient, dimensionless

T_{bat} Solar photovoltaic cell temperature, ℃

$NOCT$ Nominal operating temperature of solar photovoltaic cells, ℃

P_{spv} Solar photovoltaic cell power generation under standard conditions, kW

v Instantaneous wind speed, m/s

V_{ci} The cut-in air velocity of the fan, m/s

V_{co} The cut-out air velocity of the fan, m/s

V_r Rated wind speed of the fan, m/s

C_p Power factor of the fan, dimensionless

ρ_a Air density, kg/m³

η_{wt} Fan efficiency, dimensionless

A_{wt} Area swept by the blades of wind turbine, m²

P_{elz} Power of electrolysis tank, kW

η_{elz} Electrolysis tank efficiency

U_{elz} Operating voltage of the electrolysis tank, V

F Faraday constant, C/mol

$M_{H_2}^{in}$ Mass flow rate of hydrogen produced in the electrolysis tank, g/s

T_c Temperature of hydrogen, K

η_c Compressor efficiency, dimensionless

k Specific heat ratio of hydrogen, dimensionless

r_c Pressure ratio in the compressor, dimensionless

T_{H_2} Temperature in the hydrogen storage tank, K

P_{H_2} Pressure in hydrogen storage tank, MPa

R Ideal gas constant, J/(mol·K)

T_{FC} Fuel cell temperature, K

T_{ref} Fuel cell reference temperature, K

P_{H_2} Hydrogen partial pressure, Pa

P_{O_2} Oxygen partial pressure, Pa

λ_{air} Air chemistry measure, dimensionless

i_{FC} Current density of PEMFC, A/cm²

C_{O_2} Oxygen concentration on catalyst surface, mol/m³

$\zeta_1, \zeta_2, \zeta_3, \zeta_4$ Activation factor for fuel cells, dimensionless

P_{ASHP} Rated power of air source heat pumps, kW

ε Frost defrost loss factor, dimensionless

α, β, γ Coefficients related to COP of air source heat pumps, dimensionless

Δt Time step,h

C Specific heat capacity of water, kJ/(kg·K)

ρ_w Density of water, kg/m³

V_{tank} Volume of heat storage tank, m³

Q_{loss} Heat loss from heat storage tank, kW

U_{loss} Heat loss coefficient, kJ/(h·m²·K)

A_{tank} Cross-sectional area of heat storage tank, m²

h_{tank} Height of heat storage tank, m

c_p Specific heat capacity of hydrogen at constant pressure, kJ/(kg·K)

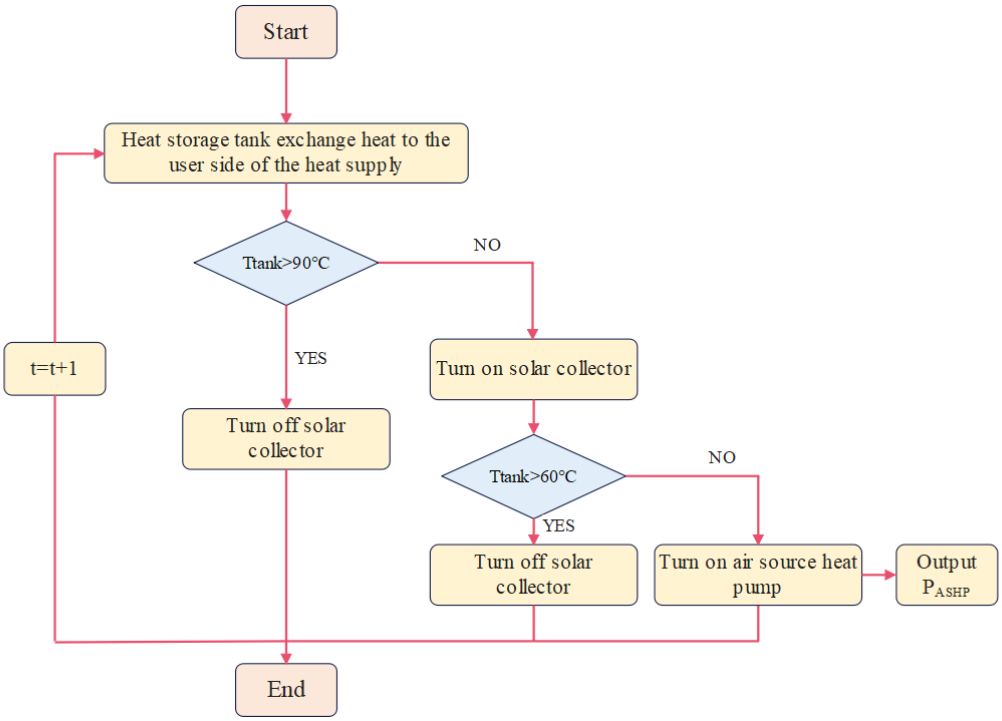

Figure 2. Operation strategy of heat system.

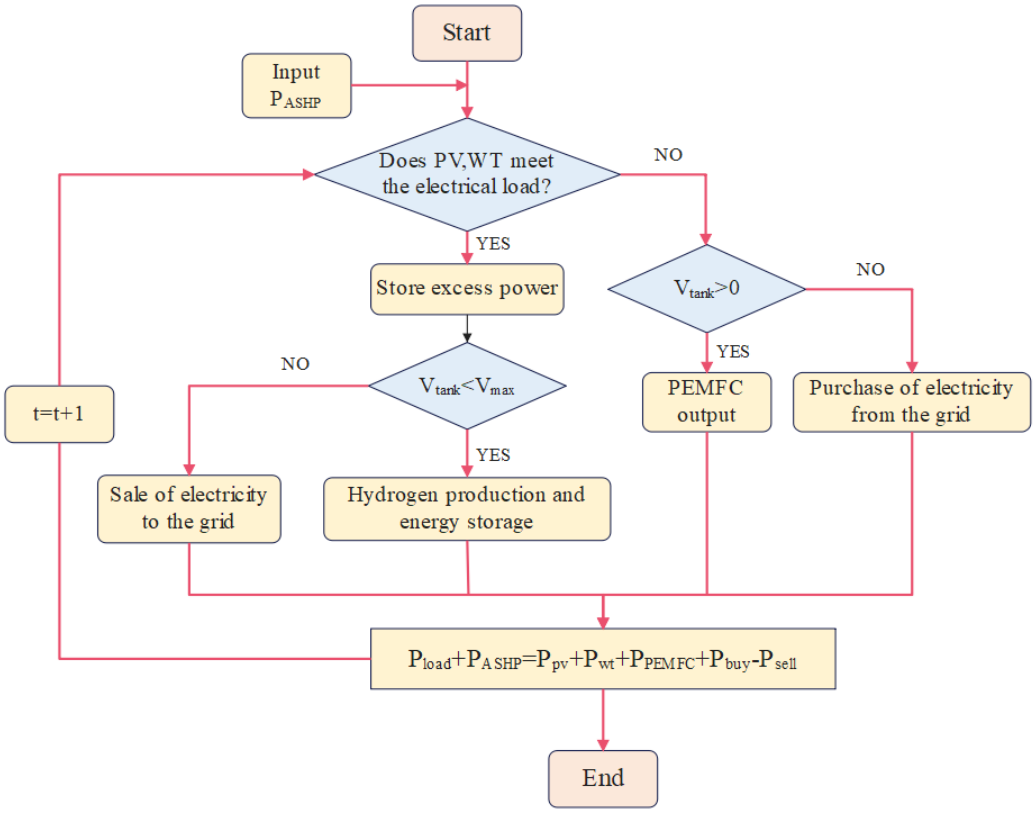

Figure 3. Operation strategy of electricity system.

Fig.3, where the electricity usage of the air source heat pump constitutes a portion of the overall power load. Solar photovoltaic cells and wind turbines primarily cater to the electricity needs. When the electricity produced by these renewable sources surpasses the building's power consumption, the surplus energy is used by an electrolysis tank to produce hydrogen, which is then stored for future use. Should the hydrogen tanks reach their full capacity, any additional excess power is sold back to the grid. Conversely, if the generated renewable energy falls short of satisfying the electrical load, the stored hydrogen is utilized by the PEMFC to generate the needed electricity. In instances where the hydrogen supply is insufficient to meet the demand, the system procures additional power from the grid to ensure a continuous power supply.

4. TWO-LAYER COLLABORATIVE OPTIMIZATION MODEL

4.1 Model idea

The complexity of system load types and the interplay between energy conversion inputs and outputs prompt the transition from traditional single-layer models to a more sophisticated two-layer collaborative optimization model. This model leverages the distinct advantages of integrating economic and environmental considerations into the planning process.

In the upper layer, an optimal configuration model for the integrated energy system is developed, simultaneously addressing economic and

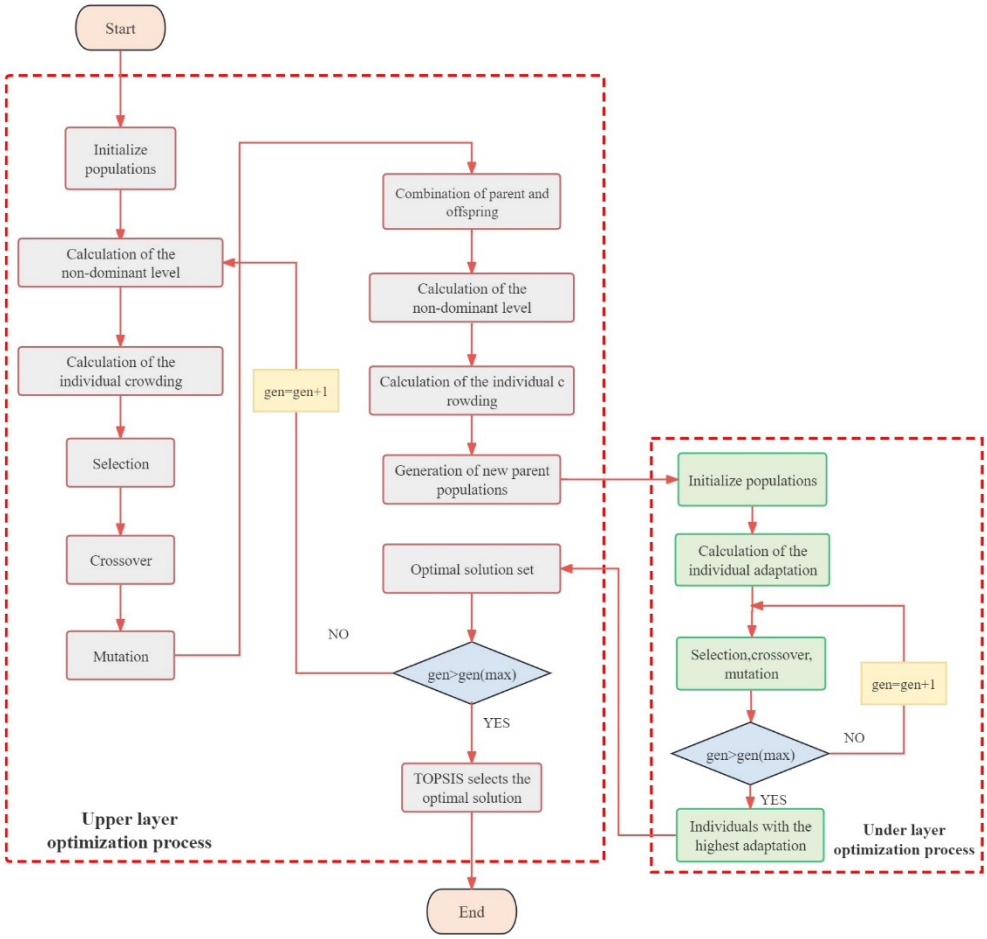

Figure 4. Flowchart of two-layer collaborative optimization model.

environmental objectives. Utilizing the NSGA-II algorithm, this layer identifies a Pareto optimal solution set that balances these objectives, establishing a synergy between the often conflicting goals of economy and environmental protection. The solutions, specifying component capacities, are then passed down to the lower layer.

The lower layer focuses on energy saving through a single-objective optimization model. It takes the upper layer's optimal solution set as its starting point, employing a genetic algorithm to refine the search iteratively (with a completion criterion of 50 generations) until the optimal solution is identified. This solution is then fed back to the upper layer for further multi-objective optimization. This iterative process continues, with the NSGA-II algorithm cycling through to its final generation (100 generations), culminating in a global Pareto-optimal solution set for the entire system.

The selection of the optimal global solution is finalized using the TOPSIS method, based on a multi-objective criterion with equal weightage assigned to each objective. This process flow is depicted in Fig.4, illustrating a structured approach to achieving a balanced and optimal system configuration.

4.2 Objective function

The selection of the optimization objective plays a crucial role in the optimization process of distributed energy system, which is directly related to the accuracy and effectiveness of the final optimization results. This is because the distributed energy system itself has the characteristics of complexity, multiplicity and dynamics, and the selection of its optimization objective not only needs to take into account the economic benefits of the system, energy efficiency and other macro factors, but also needs to take into account the environmental impact, social effects, and system reliability and other micro levels. Therefore, in the optimization study of distributed energy systems, how to scientifically and reasonably determine the optimization objectives becomes a key factor affecting the system optimization results and the overall performance improvement of the system.

4.2.1 Upper layer objective function

The objective optimization function of the upper layer will consider the economic and energy saving of the system comprehensively. The economic cost has always been the primary factor to be considered in system design, so the annualized aggregate cost (EAC) of the distributed hybrid CHP system is selected as the first optimization objective. The calculation process is as follows:

$$EAC = C_C * CRR + C_m \tag{40}$$

$$CRR = \frac{i(1+i)^n}{(1+i)^n - 1} \tag{41}$$

$$C_C = C_{pv} * P_{spv} + C_{hss} * V_{H_2} + C_{wt} * A_{wt} + C_{SC} * A_{SC} + C_{ASHP} * P_{ASHP} + C_{wtank} * V_{wtank} \tag{42}$$

$$C_m = C_s + C_g \tag{43}$$

$$C_s = C_{mpv} * P_{spv} + C_{mhss} * V_{H_2} + C_{mwt} * A_{wt} + C_{mSC} * A_{SC} + C_{mASHP} * P_{ASHP} + C_{mwtank} * V_{wtank} \tag{44}$$

$$C_g = pricebuy * \sum_{t=1}^{8760} \left(\left| E_{grid}^{in,t} \right| \right) - pricesell * \sum_{t=1}^{8760} \left(\left| E_{grid}^{out,t} \right| \right) - pension * P_{spv} \tag{45}$$

Where, C_C is the annualized initial investment,\$; C_m is the annualized maintenance cost,\$; CRR is the capital recovery rate, the factor is the inverse of the present value of the annuity, indicating that the system in the life cycle of the investment in the years of the year should be recouped, dimensionless; i for the current interest rate, the number of interest periods is equal to the number of years representing the

equipment's lifecycle in this study, dimensionless; n is the number of interest periods, years; C_s for the maintenance cost of the system,$; C_g for revenues or expenses arising from the purchase and sale of electricity ; C_{pv} for the investment cost of solar photovoltaic cells, $; C_{mpv} for the maintenance cost of solar photovoltaic cells, $; C_{hss} for the investment cost of hydrogen storage-fuel cell system, $; C_{mhss} for the maintenance cost of hydrogen storage-fuel cell system, $; C_{wt} for the investment cost of wind turbines, $; C_{mwt} for the maintenance cost of wind turbines, $. C_{SC} for the investment cost of solar collectors,$; C_{mSC} for the maintenance cost of solar collectors,$; C_{ASHP} for the investment cost of air-source heat pumps,$; C_{mASHP} for the maintenance cost of air source heat pumps,$; C_{wtank} for the investment cost of heat storage tanks,$; C_{mwtank} for the maintenance cost of heat storage tanks,$; $pricebuy$ for the price at which the system buys electricity from the grid,$; $pricesell$ is the price at which the system sells electricity to the grid,$; $pension$ is subsidy established by the government to foster the adoption of renewable energy sources,$; E_{grid}^{in} is the amount of electricity purchased by the system from the grid at time t, kW; E_{grid}^{out} is the amount of electricity sold by the system to the grid at time t, kW.

Different from the traditional cogeneration system using boiler or gas turbine as the power equipment, the PEMFC-based cogeneration system adopts hydrogen as the fuel for hydrogen production and compression, and the pollutants emitted in the process of hydrogen production and compression are mainly GHGs, including carbon dioxide (CO2), methane (CH4), and nitrous oxide (N2O), so that the total GHG emissions can be selected as the total pollutant emissions of the system, and the calculation process is as follows:

$$Emissions = LHV_{H_2} \times GHG \tag{46}$$

Where, LHV_{H_2} is the total calorific value of hydrogen consumed by the system, MJ; and GHG is the greenhouse gas emissions, g·MJ^{-1}.

4.2.2 Lower level objective function

For an energy system, if the primary energy utilization is higher, this indicates that the thermal performance of the system is better, so the primary energy utilization (PER) is selected as the second optimization objective, and the calculation process is as follows:

$$PER = \frac{Q_{recovered\_heat} + P_{el}}{Q_{in}} \tag{47}$$

Where, $Q_{recovered\_heat}$ is the amount of waste heat recovered from the system, kW; P_{el} is the amount of electricity generated by the system, kW; and Q_{in} is the energy input to the system, kW.

The optimization objective is to minimize EAC and $Emissions$,while maximizing PER , i.e. as follows:

$$\begin{cases} max\ PER \\ min\ EAC, Emissions \end{cases} \tag{48}$$

4.3 Decision variables and constraints

The objective of the study presented in this chapter is to determine the optimal installed capacity for each component through the integration of operation strategies. Consequently, the decision variable under consideration is the installed capacity of each device within the system, as outlined in equation (49). The constraints primarily encompass the installed capacity or size limitations of the components, along with energy balance constraints. These limitations should be determined based on practical considerations, as demonstrated in equation (50).

Decision variables:

$$X = [P_{spv}, V_{tank}, A_{wt}, A_{SC}, P_{ASHP}, n_{FC}, V_{H_2}] \tag{49}$$

Constraints:

$$\begin{aligned} &0 \le P_{spv} \le P_{spv,max};\ 0 \le P_{ASHP} \le P_{ASHP,max} \\ &0 \le V_{tank} \le V_{tank,max};\ 0 \le n_{FC} \le n_{FC,max} \\ &0 \le A_{wt} \le A_{wt,max};\ 0 \le V_{H_2} \le V_{H_2,max} \\ &0 \le A_{SC} \le A_{SC,max};\ T_{tank,min} \le T_{tank} \le T_{tank,max} \end{aligned} \tag{50}$$

Where, P_{spv} is the rated power of the solar photovoltaic cell, kW; V_{tank} is the volume of the heat storage tank, m^3; A_{wt} is the swept area of the wind turbine blades, m^2; A_{SC} is the covered area of the solar collector, m^2; P_{ASHP} is the rated power of the air-source heat pump, kW; n_{FC} is the number of the fuel cell blocks, blocks; V_{H_2} is the volume of the hydrogen storage tank, m^3.

During the computation, the above decision variables are adjusted at each iteration according to the constraints of the master function. If the value of the variable exceeds the upper limit of the constraint, it will be reassigned to the maximum value allowed. Conversely, if the value of the variable falls below the lower limit of the constraint, it will be reassigned to the minimum value allowed. This ensures that the decision variable always satisfies the constraints of the master function.

Energy conservation constraints for electrical systems:

The ultimate purpose of designing a distributed hybrid CHP system is to satisfy the power and heat demand on the user's side, and in the operation phase of the system, the output power of the system at time t plus the power interactively purchased or sold from the grid and the building loads should be kept equal, as shown in equation (51):

$$P_{pv}(t) + P_{wt}(t) + P_{PEMFC}(t) + E_{grid}^{in}(t) - E_{grid}^{out}(t) = P_{load}(t) + P_{ASHP}(t) \tag{51}$$

Where, P_{pv} is the solar photovoltaic output, kW; P_{wt} is the wind turbine output, kW; P_{PEMFC} is the fuel cell output, kW; P_{load} is the building load, kW; and P_{ASHP} is the air source heat pump output, kW.

Energy conservation constraints for heat systems:

Similarly, the heat equilibrium is given by as shown in equation (52):

$$Q_{SC}(t) + Q_{ASHP}(t) + Q_{tank}(t) = Q_{load}(t) + Q_{loss}(t) \tag{52}$$

Where, Q_{SC} is the output of solar collector, kW; Q_{ASHP} is the output of air heat pump, kW; Q_{tank} is the output of heat storage tank, kW; Q_{load} is the heat generated or consumed by the building, kW; Q_{loss} is and the heat loss of heat storage tank at each moment, kW.

5. SYSTEM OPTIMIZATION ANALYSIS

In the system studied in this paper, the time interval is set to 1 hour, i.e., it is assumed that the data remain constant during each hourly time period. Therefore, the total number of data points in a year is 8760, which provides sufficient data support for accurate analysis. Once data on the electricity and heat demand in a given area are available, as well as local renewable energy conditions (e.g., wind speed and solar radiation intensity), combined with the fixed parameter values for each component in the system, optimization analyses can be initiated.

In the optimization process, with $P_{spv}, V_{tank}, A_{wt}, A_{SC}, P_{ASHP}, n_{FC}, V_{H_2}$ as the decision variable, combined with the prescribed system operation strategy, by substituting equations (1-39), the output data of each component at different time periods and determined by the decision variable can be derived. These data not only reflect the performance of the components, but also provide the basis for the subsequent objective function construction.

In order to realize the economic, environmental and energy saving objectives of this system, three objective functions are constructed by combining the output data of each component, which fully consider the economic cost, energy consumption and environmental impact of each component. On this basis, the objective functions are optimized to derive the Pareto optimal solution set under the constraints defined in equations (50-52) using a two-layer collaborative optimization model.

As mentioned above, optimal solutions need to be obtained from the Pareto optimal solution set based on different metrics in the multi-objective optimization problem. In this paper, the three metrics from the optimization model are EAC, Emissions and PER. Since every solution in the Pareto solution set can be the final solution of the energy system, a solution selection process is required in determining the final capacity solution of the component. Researchers have developed a large number of solution selection methods. The distance between superior and inferior solutions method (TOPSIS) is a method for selecting the

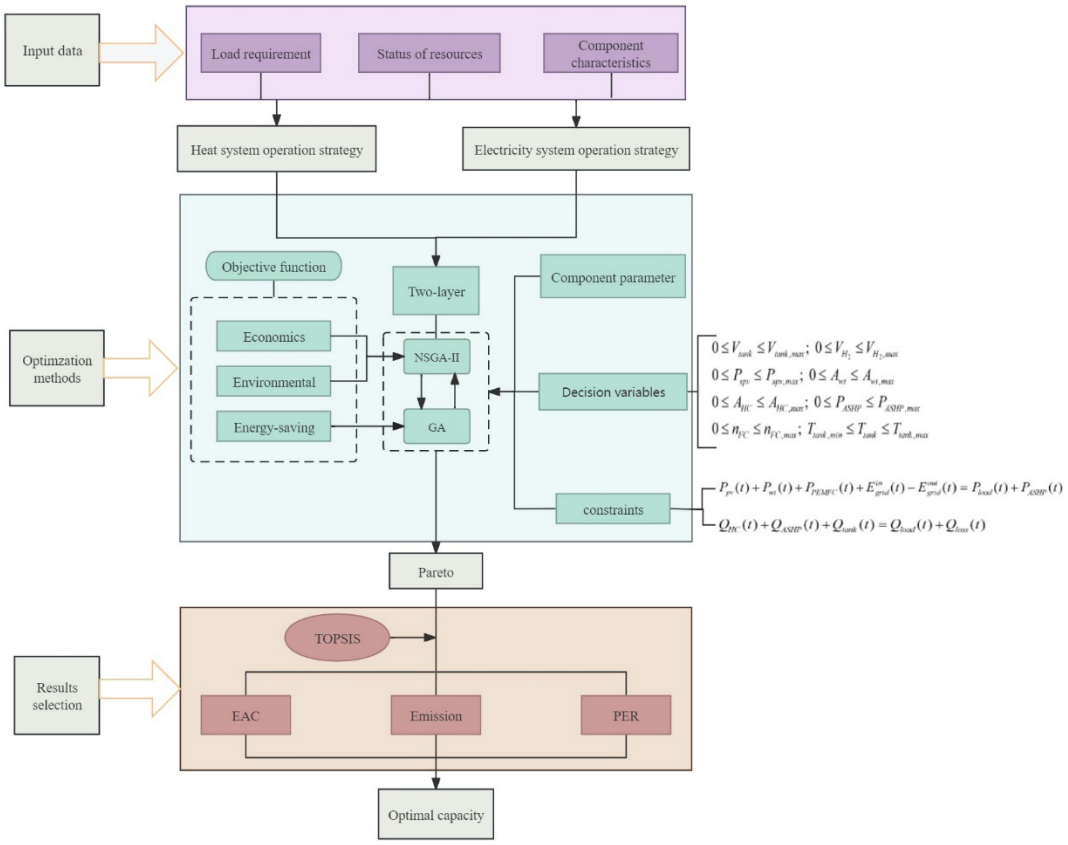

Figure 5. System optimization process.

optimal solution based on the distance between the ideal solution and the desired solution. The ideal and undesirable solutions are calculated using Pareto solution set and indicator preferences. In this paper, the weights assigned to each evaluation objective are equivalent.

The optimization process aims to achieve the comprehensive optimization of multiple objectives, i.e., to find the best balance between economy, environmental protection and energy saving. After optimization, the values of the decision variables will represent the best capacity configuration of each component, thus achieving the optimization of the overall system performance. The specific optimization process is shown in Fig. 5:

6. CONCLUSION

In this study, we introduce a multi-objective optimization framework for a hybrid energy system that prioritizes economic viability, environmental protection, and energy efficiency. Our system integrates solar and wind power with energy storage solutions, centering around a proton exchange membrane fuel cell (PEMFC) and utilizing hydrogen as the primary storage medium. This setup not only significantly cuts carbon and pollutant emissions but also offers a viable path towards environmental sustainability and the advancement of clean energy.

We've devised a dynamic energy management strategy to address fluctuations in energy supply. During periods of surplus, excess electricity is converted into hydrogen through electrolysis, with the option to sell back to the grid. Conversely, in times of shortfall, the PEMFC taps into the hydrogen reserve to fulfill energy demands, with the grid acting as a backup source if hydrogen levels are low. This bidirectional grid interaction enhances the system's adaptability and optimizes energy usage.

Our proposed dual-layer collaborative optimization model navigates the trade-off between minimizing costs and maximizing energy efficiency. By employing the NSGA-II algorithm alongside genetic algorithms, we provide users with a spectrum of sophisticated and tailored system configurations. This approach outperforms traditional single-objective optimization and dual-layer singular objective optimization by ensuring optimal solutions while accelerating the search process and boosting overall efficiency, allowing for quicker identification of the best system configurations.

Looking ahead, we aim to delve deeper into the synergies and dynamics between various energy systems, considering the intricacies of grid architecture and distributed computing algorithms. This exploration is poised to enhance the efficiency and reliability of energy systems, pushing the envelope on sustainable energy solutions and contributing significantly to the pursuit of a sustainable energy future.

REFERENCES

[1] Feng, P., Chen, X., Xu, T. 2020. A Review of Microgrid Key Technology Research. Hydropower and Pumped Storage, 6(03), 45-49.

[2] Li, C., Wang, N., Dou, X., et al. 2023. Review and Prospect of Multi-Energy Complementary Distributed Energy System Integration Research. Chinese Journal of Electrical Engineering, 43(18), 7127-7150.

[3] Kamel, M. A., Elbanhawy, A.Y., and Abo El-Nasr, M. 2019. A Novel Methodology to Compare Between Side-By-Side Photovoltaics and Thermal Collectors Against Hybrid Photovoltaic Thermal Collectors. Energy Conversion and Management, 202, 112196

[4] Cha, Y. X., Wu, T., Peng, J. C., et al. 2020. Optimized Scheduling of Hybrid Power Generation System with Renewable Energy Based on Multi-Objective Multi-Task Evolutionary Algorithm. Journal of North China Electric Power University (Natural Science Edition), 47(01), 70-78.

[5] Yang, X., Wang, R., Yu, C., et al. 2023. Optimal Scheduling of Distributed Energy System Based on Improved Gray Wolf Optimization Algorithm. Inner Mongolia Power Technology, 41(01), 26-33.

[6] Jiang, Z., Liu, Z., Xu, J., et al. 2021. A Two-Layer Cooperative Optimization Method for Combined Cooling, Heat and Power Supply System Taking into Account Wind and Solar Storage. Electric Power Construction, 42(08), 71-80.

[7] Bian, X., Shi, Y., Bui, C., et al. 2021. Optimization of Two-Layer

Synergistic Configuration of Regional Integrated Energy System Taking into Account Economic and Reliability Factors. Journal of Electrotechnology, 36(21), ,4529-4543.

[8] Dong, L., Wu, Y., Zhang, T., et al. 2023. Reinforcement Learning-Based Two-Layer Optimization Method for Active Distribution Networks Containing Intelligent Soft Switches. Power System Automation, 47(06), 59-68.

[9] Cai, W., Li, X., Maleki, A., Pourfayaz, F., Rosen, M. A., Alhuyi Nazari, M., Bui, D. T. 2020. Optimal Sizing and Location Based on Economic Parameters for an Off-Grid Application of a Hybrid System with Photovoltaic, Battery and Diesel Technology. Energy, 201, 117480.

[10] Evans, D. L. 1981. Simplified Method for Predicting Photovoltaic Array Output. Solar Energy, 27(6), 555–560.

[11] Maleki, A. 2018. Design And Optimization of Autonomous Solar-Wind-Reverse Osmosis Desalination Systems Coupling Battery and Hydrogen Energy Storage by an Improved Bee Algorithm. Desalination, 435, 221–234.

[12] Shaygan, M., Ehyaei, M. A., Ahmadi, A., Assad, M. E. H., Silveira, J. L. 2019. Energy, Exergy, Advanced Exergy and Economic Analyses of Hybrid Polymer Electrolyte Membrane (PEM) Fuel Cell and Photovoltaic Cells to Produce Hydrogen and Electricity. Journal of Cleaner Production, 234, 1082– 1093.

[13] Barbir, F., Gómez, T. 1997. Efficiency And Economics of Proton Exchange Membrane (PEM) Fuel Cells. International Journal of Hydrogen Energy, 22(10), 1027– 1037.

[14] Keshavarzzadeh, A. H., Ahmadi, P., Safaei, M. R. 2019. Assessment and Optimization of an Integrated Energy System with Electrolysis and Fuel Cells for Electricity, Cooling and Hydrogen Production Using Various Optimization Techniques. International Journal of Hydrogen Energy, 44(39), 21379–21396.

[15] Safari, F., Dincer, I. 2018. Assessment And Optimization of an Integrated Wind Power System for Hydrogen and Methane Production. Energy Conversion and Management, 177, 693–703.

[16] Siddiqui, O., Dincer, I. 2021. Optimization of a New Renewable Energy System for Producing Electricity, Hydrogen and Ammonia. Sustainable Energy Technologies and Assessments, 44, 101023.

[17] Al-Baghdadi, M. A. R. S. 2005. Modelling Of Proton Exchange Membrane Fuel Cell Performance Based on Semi-Empirical Equations. Renewable Energy, 30(10), 1587–1599.

[18] Shahverdian, M. H., Sohani, A., Sayyaadi, H. 2022. A 3E Water Energy Nexus Based Optimum Design for A Hybrid PV-PEMFC Electricity Production Systems for Off-Gird Applications. Energy Conversion and Management, 267, 115911.

[19] Qureshy, A. M. M. I., Dincer, I. 2021. Investigation of a Solar Hydrogen Generating System Design for Green Applications. Applied Thermal Engineering, 193, 117008.

[20] Miansari, M., Sedighi, K., Amidpour, M., Alizadeh, E., Miansari, M. 2009. Experimental and Thermodynamic Approach on Proton Exchange Membrane Fuel Cell Performance. Journal of Power Sources, 190(2), 356–361.